Journal of Hazardous Materials 184 (2010) 1–5

Contents lists available at ScienceDirect

Journal of Hazardous Materials

journal homepage: www.elsevier.com/locate/jhazmat

Preparation, characterization and photocatalytic activity of a novel composite photocatalyst: Ceria-coated activated carbon

Chao Wang[a,b,c], Yanhui Ao[a,b,c,*], Peifang Wang[a,b,c], Jun Hou[a,b,c], Jin Qian[a,b,c]

[a] Key Laboratory of Integrated Regulation and Resource Development on Shallow Lakes, Ministry of Education, Hohai University, Nanjing, 210098, China
[b] College of Environmental Science and Engineering, Hohai University, Nanjing, 210098, China
[c] State Key Laboratory of Hydrology-Water Resources and Hydraulic Engineering, Hohai University, Nanjing, 210098, China

ARTICLE INFO

Article history:
Received 31 January 2010
Received in revised form 1 June 2010
Accepted 9 July 2010
Available online 16 July 2010

Keywords:
Photocatalysis
Ceria
Activated carbon
Composite
4-CP

ABSTRACT

In the present work, a novel composite photocatalyst ceria-coated activated carbon (CCAC) was prepared by a facile method. The composite photocatalyst was characterized by X-ray diffraction (XRD), Brunauer–Emmett–Teller (BET), scanning electron microscopy (SEM) and photocatalytic degradation of 4-chlorophenol (4-CP). A synergy effect for 4-CP degradation was observed because the activated carbon (AC) with strong adsorbent activity provided sites for the adsorption of 4-CP. Then, the adsorbed 4-CP can migrate continuously onto the surface of ceria particles and then degraded at there. Hydroquinone (HQ) and benzoquinone (BQ) were found to be the main intermediates of the photocatalytic 4-CP degradation with ceria or CCAC by HPLC measurement. The results suggested that the same reaction mechanism occurred in the presence of ceria or titania.

1. Introduction

In recent two decades, heterogeneous photocatalysis has emerged as an efficient technology to purify air and water [1–6]. This technique is based upon the use of UV irradiated semiconductors, generally titanium dioxide (TiO_2) which is one of the most promising semiconductor photocatalysts, to destroy various organic pollutants. Titanium dioxide has been extensively studied for environmental purification applications, due to its good characteristics of powerful oxidation strength, chemical stability, nontoxicity and inexpensiveness. However, it also shows some disadvantages such as: formation of toxic by-products and deactivation of the photocatalysts, thus it cannot be long term utilized [7–9]. Consequently, there are considerable attentions on the development of alternative photocatalyst with improved photocatalytic activity or longer stability during prolonged application [10–12].

Ceria is an inexpensive material, and has some properties like titania such as wide band gap, nontoxicity, and high stability. Therefore, ceria has been selected as a component to prepared composite oxides or as a dopant to improve the performances of titania photocatalyst [13–16]. More recently, there are also some articles reported the investigation of water-splitting for the generation of hydrogen gas and photocatalytic degradation of organic contaminants [17–20].

However, all the existent studies investigated only the photocatalytic activity of pure ceria, while the photocatalytic efficiency of pure ceria still cannot fulfill the practical application in wastewater treatment. The objectives of this study were to exploit novel ceria-based composite photocatalyst with enhanced photocatalytic activity. Therefore, we associated the adsorption activity of activated carbon (AC) with the photocatalytic activity of ceria. In the present work, we prepared ceria-coated activated carbon composite photocatalyst. The adsorption and photocatalytic properties of as-prepared composite were determined by adsorbing and degrading of 4-chlorophenol (4-CP) in aqueous solution. Results showed that the adsorption and photocatalytic activity enhanced a lot compared to the pure ceria or titania P25.

2. Materials and methods

2.1. Materials

All chemicals were of reagent grade or higher purity, and were used without further purification. $Ce(NO_3)_3{\cdot}6H_2O$, $NH_3{\cdot}H_2O$ and 4-CP were purchased from Shanghai Sinopharm Chemical Reagent Co., Ltd., China. Activated carbon with specific surface area around 1100 $m^2\,g^{-1}$ was purchased from Shanghai Acti-

* Corresponding author at: State Key Laboratory of Hydrology-Water Resources and Hydraulic Engineering, Hohai University, Nanjing, 210098, China. Tel.: +86 25 83787330; fax: +86 25 83787330.
E-mail address: andyao@seu.edu.cn (Y. Ao).

0304-3894/$ – see front matter © 2010 Elsevier B.V. All rights reserved.
doi:10.1016/j.jhazmat.2010.07.034

vated Carbon Ltd. Ultrapure water was used throughout this study.

2.2. Sample preparation

0.01 mol $Ce(NO_3)_3{\cdot}6H_2O$ was dissolved into 100 mL ultrapure water. Afterwards, 5 mL $NH_3{\cdot}H_2O$ was added dropwise into the above solution under vigorous stirring. After 2 h, 1.72 g activated carbon was added into the reaction system, and the stirring was last for another 12 h. The obtained sample was centrifuged and washed by water for five times before it was dried at 60 °C under vacuum. Finally, the sample was calcined at 300 °C for 6 h.

2.3. Characterization

The structure properties were determined by X-ray diffractometer (XD-3A, Shimadazu Corporation, Japan) using graphite monochromatic copper radiation (Cu Kα) at 40 kV, 30 mA over the 2θ range 20–80°. The morphologies were characterized with a scanning electron microscopy (SEM). Brunauer–Emmett–Teller (BET) surface area measurements were carried out by N_2 adsorption at 77 K using an ASAP2020 instrument. The total pore volume was calculated from the amount of nitrogen adsorbed at relative pressure of 0.975. The HPLC system was Agilent 1100 with tunable absorbance detector adjusted at 220 nm for the detection of 4-CP. A reverse-phase column (length, 250 mm; internal diameter, 4.6 mm) Aglient Eclipse XDB-C18 was used. The mobile phase was composed of methanol and deionized doubly distilled water. The v/v ratio CH_3OH/H_2O was 50/50 and the flow rate was 1 mL min^{-1}.

2.4. Adsorption experiments

For the adsorption measurements, 0.05 g ceria, P25 (or 0.1 g CCAC) was added to 100 mL of freshly prepared 4-CP solutions of known concentration in the range 10–100 mg L^{-1} at natural pH. The suspensions were sonicated for 5 min and then stirred for 1 h at room temperature in the dark to reach adsorption–desorption equilibrium. After filtration through a Millipore filter membrane (0.22 μm), the sample was taken to determine the concentration of 4-CP on a UV–vis spectrophotometer.

2.5. Photocatalytic experiment

In an ordinary photocatalytic test performed at room temperature, 0.1 g the obtained composite photocatalyst was added into 100 mL 4-CP aqueous solution whose concentration was 100 mg L^{-1}. The suspension was stirred in the dark for 1 h to reach adsorption–desorption equilibrium. The irradiation was provided by ultraviolet lamp (20 W, with a wavelength peak at 365 nm). Samples of the suspension (5 mL) were removed at regular intervals for analysis.

3. Results and discussion

3.1. Characterization of the photocatalyst

Phase structures of as-prepared sample were investigated by the X-ray diffraction (XRD) analysis, and the result is shown in Fig. 1. It can be seen that all the diffraction peaks can be indexed as a face-centered cubic phase CeO_2 (JCPDS no. 34-394). The diffraction peaks at 2θ values of 28.5°, 33.1°, 47.4° and 56.2° can be assigned to the reflections of (1 1 1), (2 0 0), (2 2 0) and (3 1 1) planes of cubic CeO_2, respectively. The average crystallite sizes of as-prepared samples can be calculated by applying the Debye–Scherrer formula

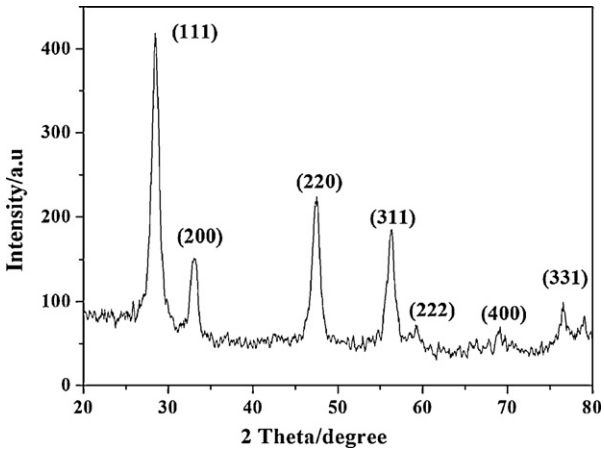

Fig. 1. XRD of the as-prepared CCAC.

on the diffraction peaks: [21]

$$D = \frac{K\lambda}{\beta \cos\theta} \quad (1)$$

where D is the crystalline size, λ the wavelength of X-ray radiation (0.1541 nm), K the constant usually taken as 0.89, and β is the full peak width (in radians) at half-maximum height after subtraction of equipment broadening, and θ is the Bragg angle of the X-ray diffraction peak. Using the equation, the calculated crystalline size of CeO_2 in CCAC is 8.3 nm.

BET isotherm plots of CCAC and CeO_2 are shown in Fig. 2. From the figure we can see that a clear hysteresis at high relative pressure is observed for both samples, which is related to capillary condensation associated with large pore channels, indicating the presence of mesopores (type IV). From the plot of CCAC, we can also see that there existed some micro-pores. The BET surface areas are 522.1 and 112.6 $m^2\ g^{-1}$ for CCAC and CeO_2, respectively. The pore size distribution calculated from the desorption branch of the isotherm are also presented in Fig. 3. The results also confirmed the presence of mesopores. The pore centered at 7.05 nm, 3.72 and 6.18 nm for CeO_2 and CCAC, respectively. The pores centered at 6.18 nm may be newly formed by ceria nanoparticles agglomerate on the activated carbon.

Fig. 4(a) shows the SEM image of CCAC. From the image we can see that ceria particles are loaded on the surface of activated carbon evenly with a few aggregations. In Fig. 4(b), we also show the magnified image of CCAC, from which we can see the diameters of ceria particles are ranged from 30 to 40 nm. The value is extremely different from the XRD calculated size. This difference

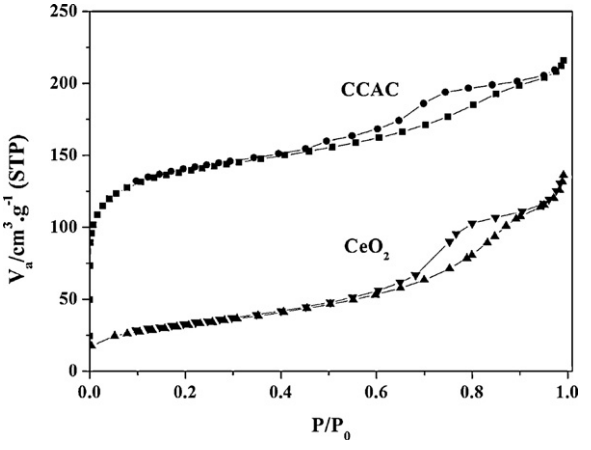

Fig. 2. BET isotherm plot of CCAC and CeO_2.

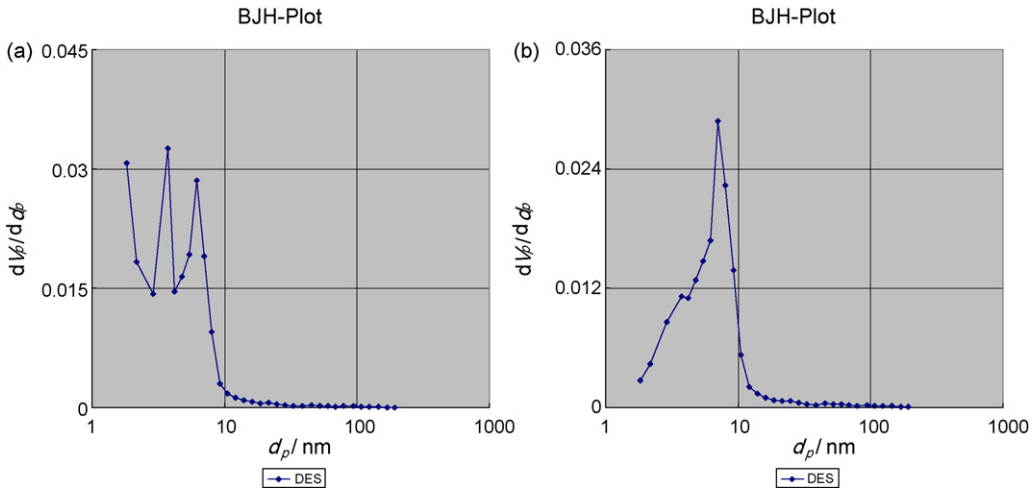

Fig. 3. Pore diameter distribution of (a) CCAC and (b) CeO_2.

may be attributed to the aggregation of single ceria crystalline into bigger sized particles.

3.2. Adsorption capacity of the photocatalyst for 4-CP

Adsorption of pollutants on the semiconductor surface is an important parameter for the photocatalytic activity in heterogeneous photocatalysis. The isothermal adsorption curves of 4-CP (100 mg L^{-1}) on different photocatalysts are shown in Fig. 5. From the figure we can know that most adsorption of 4-CP occurred in the initial 15 min. A series of adsorption experiments (in the range 10–100 mg L^{-1}) were carried out to investigate the adsorption equilibrium constants and the extent of saturated adsorption. The conventional Langmuir isotherm model with a surface coverage θ varying as: $\theta = n_{ads}/n_T = K_{ads}C/(1 + K_{ads}C)$ was used to determine the total number of adsorption sites n_T and the constant K_{ads} from the linear transform $(1/n_{ads}) = f(1/c)$ obtained with correlation coefficients close to 0.99. The corresponding values are given in Table 1. It can be seen from Table 1 (column 3) that the total number of adsorption sites of ceria-coated activated carbon is slightly smaller than that of activated carbon. Similarly, the amount of 4-CP adsorbed on different samples follows the same trend as the case of 100 mg L^{-1} (Fig. 5). There is no additivity of the adsorption capacities of ceria-coated activated carbon compared to the activated

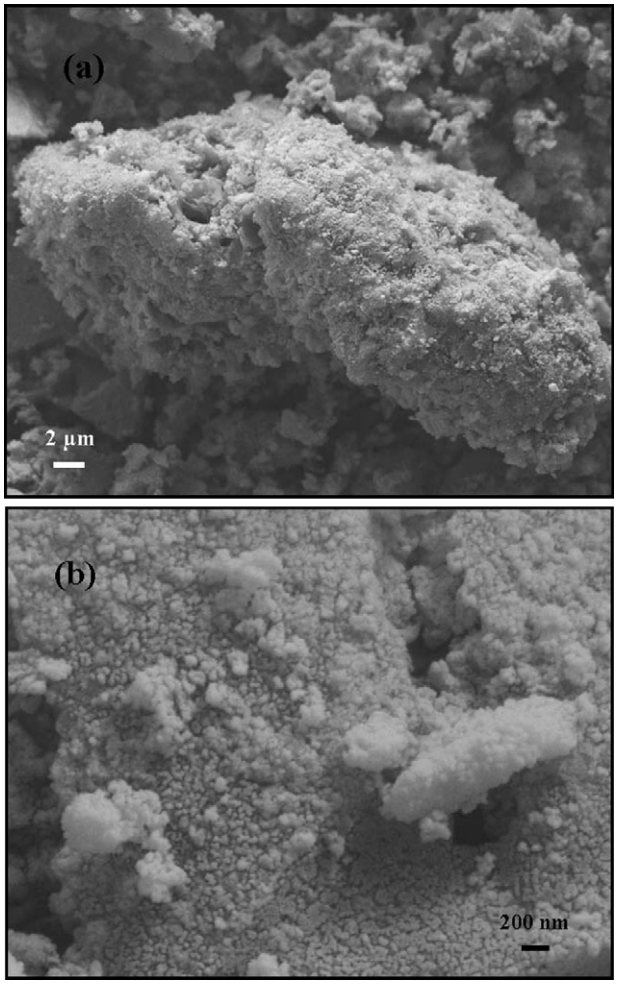

Fig. 4. SEM images of CCAC (a) low magnification, and (b) high magnification.

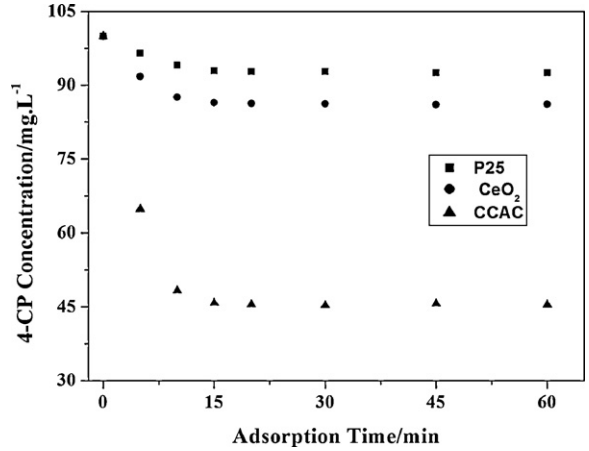

Fig. 5. Adsorption kinetic of 4-CP (100 mg L^{-1}) in the dark by different samples.

Table 1
Langmuir isotherm parameters: adsorption constant (K_{ads}) and total number of adsorption sites (n_T).

Samples	K_{ads} (L mol^{-1})	n_T (mol)
P25	1.64×10^3	9.44×10^{-6}
CeO_2	2.09×10^3	1.5×10^{-5}
AC	6.60×10^4	4.4×10^{-5}
CCAC	4.64×10^4	4.1×10^{-5}

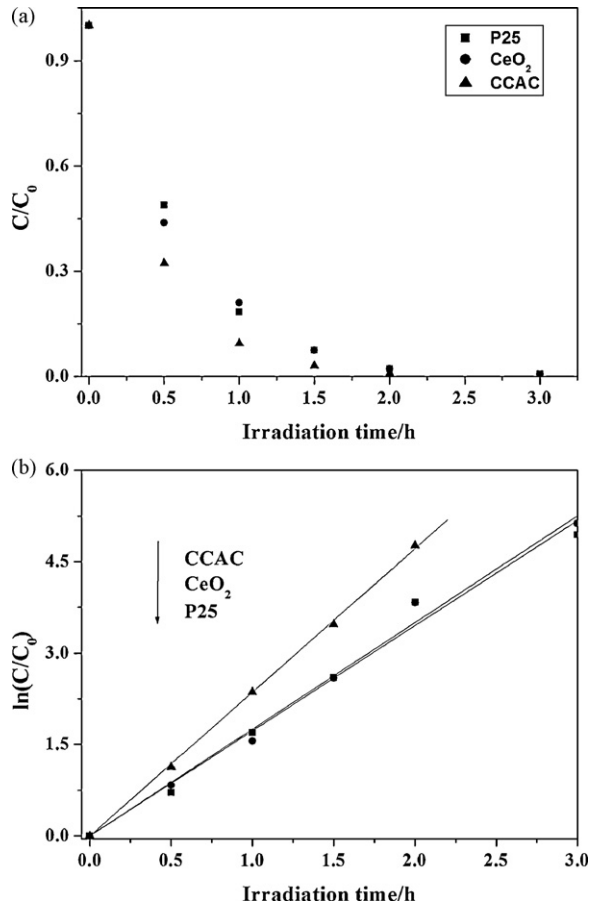

Fig. 6. Variations of (a) C/C_0 and (b) $\ln(C_0/C)$ against irradiation time in the presence of different samples.

carbon. This could be ascribed to the ceria coated on the surface or pores of the activated carbon, taking up some adsorption sites of the activated carbon. When the obtained data of adsorption parameters are compared to the values reported by Matos and co-workers [22,23], we find that our values of adsorption parameters for both P25 and activated carbon are higher than literature data. This may be ascribed to the different experiment conditions (temperature, pH, pore diameter of filtration membrane, etc.).

3.3. Photocatalytic degradation of 4-CP by the photocatalyst

Comparison of photocatalytic activity of three samples, which were commercial titania P25, pure ceria, ceria-coated activated carbon, was performed. The results are shown in Fig. 6(a), from which we can see that CCAC exhibited the highest photocatalytic activity. Furthermore, we perform a test using activated carbon without ceria loading under the same condition, and the results show that only 4% 4-CP was degraded after 3 h UV irradiation. Therefore, we can conclude that the 4-CP removal is really caused by the photocatalytic activity of ceria in the composite sample. We also investigated the kinetics of 4-CP degradation by different samples through Langmuir–Hinshelwood model:

$$-\frac{dC}{dt} = \frac{k_r K_a C}{1 + K_a C} \quad (2)$$

where $(-dC/dt)$ is the degradation rate of 4-CP, C is the 4-CP concentration in the solution, t is reaction time, k_r is a reaction rate constant, and K_a is the adsorption coefficient of the reactant. K_aC is negligible when value of C is very small. As a result, Eq. (1) can be describes a first-order kinetics. Setting Eq. (2) at the initial conditions of the photocatalytic procedure, when $t = 0$, $C = C_0$, it can be described as follows:

$$\ln\left(\frac{C_0}{C}\right) = k_{app} \times t \quad (3)$$

where k_{app} is apparent rate constant, chosen as the basic kinetic parameter for the different photocatalysts, since it enables one to determine a photocatalytic activity independent of the previous adsorption period in the dark and the concentration of 4-CP remaining in the solution [24]. The variations in $\ln(C_0/C)$ as a function of irradiation time are given in Fig. 6(b). The obtained apparent rate constants k_{app} are 1.72, 1.75 and 2.36 h^{-1} for P25, CeO_2 and CCAC, respectively. The enhanced photocatalytic activity can be ascribed to the enhanced adsorption activity of the composite photocatalyst. It can be seen from the data of adsorption of 4-CP on different samples; the adsorption constant of the composite photocatalyst much higher than that of pure CeO_2. Therefore, the 4-CP can be adsorbed onto the photocatalyst more quickly and degraded there.

Furthermore, from the data of k_{app} and K_a, we can calculated the value of reaction rate constant k_r. The calculated values were 1.05×10^{-3}, 0.84×10^{-3} and 0.51×10^{-4} mol L^{-1} h^{-1} for P25, CeO_2 and CCAC, respectively. The results show that the trend of k_r is absolutely reverse with the trend of k_{app} for the three samples. It is not surprising since that k_r reflects the decreasing rate of 4-CP in the solution, while the k_{app} reflects the decreasing rate of 4-CP in the whole system (including the 4-CP in solution and 4-CP adsorbed on the photocatalyst). Therefore, P25 shows the highest k_r value because there is the highest concentration of 4-CP remaining in the solution after the adsorption–desorption equilibrium. The above results prove ulteriorly that adsorption of pollutants on the photocatalyst surface is a key factor for the photocatalytic activity in heterogeneous photocatalysis.

3.4. Analysis of major intermediates of 4-CP

There are many papers reported on the detection for intermediates of 4-CP in the photocatalytic process by titania. However, there is no research focused on the photocatalytic degradation of 4-CP by ceria. Therefore, we investigate the photocatalytic degradation of 4-CP in the presence of ceria-coated activated carbon. We also investigate the intermediates of 4-CP in this process. It is well known that the photocatalytic degradation of 4-CP is a complex reaction process because numbers of intermediates altering with experimental conditions. According to Cheng et al. [25], the major intermediates of 4-CP degradation with carbon-modified titania under visible light were hydroquinone (HQ), benzoquinone (BQ) and hydroxyhydroquinone (HHQ). In our experiment, the detected intermediates of 4-CP degradation with ceria or CCAC under UV light irradiation were HQ and BQ. Fig. 7 shows the variations of HQ and BQ concentration against irradiation time. From the figure we can see that the amount of HQ and BQ are much higher with ceria than with CCAC. This is indicative of a higher rate of appearance and of disappearance of intermediates in the presence of irradiated CCAC, in line with what has been observed for 4-CP degradation. Furthermore, in the photocatalytic degradation of 4-CP by CCAC, the intermediates were very little as shown in Fig. 7(b). This may be ascribed to the strong adsorption activity of AC to the intermediates, which would be degraded mostly before they dissolved into aqueous solution. Therefore, the amount of intermediates was very little. For more quantitative investigation of the reaction pathway of the appearance and disappearance of the major intermediates, a comprehensive kinetic model was proposed by Alfano and co-workers [26]. In the future work, we will also investigate a comprehensive kinetic model including incident radiation, concentration of 4-CP and its intermediates by a more quantitative method.

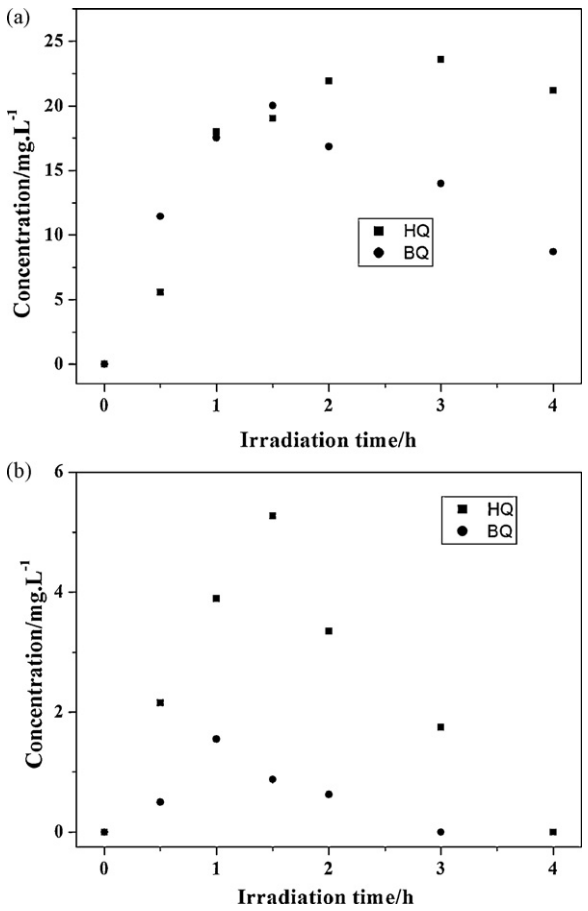

Fig. 7. Variations of intermediates concentration against irradiation time in the presence of (a) ceria and (b) CCAC.

4. Conclusion

We reported an investigation on the preparation and photocatalytic activity of a novel composite photocatalyst: ceria-coated activated carbon. Results show that such composite photocatalyst shows much higher photocatalytic activity for 4-CP degradation under UV light. The degradation intermediates of 4-CP by this photocatalyst were also investigated, and results show that the intermediates are similar with the degradation process of 4-CP in the presence of titania. This indicates that 4-CP degradation in the presence of two different types photocatalysts (ceria and titania) experiences a similar reaction pathway.

Acknowledgments

We are grateful for grants from the General Program of National Natural Science Foundation of China (no. 40871227), Basic research project of Jiangsu province (BK2008041), University Natural Science Foundation of Jiangsu Education Bureau (Peifang Wang), China Postdoctoral Science Foundation (no. 20090450133).

References

[1] A. Fujishima, T.N. Rao, D.A. Tryk, Titanium dioxide photocatalysis, J. Photochem. Photobiol. C 1 (2000) 1–21.
[2] A.L. Linsebigler, G.Q. Lu, J.T. Yates, Photocatalysis on TiO_2 surfaces: principles, mechanisms, and selected results, Chem. Rev. 95 (1995) 735–758.
[3] A. Vohra, D.Y. Goswami, D.A. Deshpande, S.S. Block, Enhanced photocatalytic disinfection of indoor air, Appl. Catal. B: 64 (2006) 57–65.
[4] N.M. Mahmoodi, M. Arami, N.Y. Limaee, N.S. Tabrizi, Kinetics of heterogeneous photocatalytic degradation of reactive dyes in an immobilized TiO_2 photocatalytic reactor, J. Colloid Interface Sci. 295 (2006) 159–164.
[5] Y.H. Ao, J.J. Xu, D.G. Fu, C.W. Yuan, A simple route for the preparation of anatase titania-coated magnetic porous carbons with enhanced photocatalytic activity, Carbon 46 (2008) 596–603.
[6] W.D. Wang, C.G. Silva, J.L. Faria, Photocatalytic degradation of Chromotrope 2R using nanocrystalline TiO_2/activated-carbon composite catalysts, Appl. Catal B 70 (2007) 470–478.
[7] R.M. Alberici, W.F. Jardim, Photocatalytic destruction of VOCs in the gas-phase using titanium dioxide, Appl. Catal. B 14 (1997) 55–68.
[8] M. Anpo, M. Takeuchi, The design and development of highly reactive titanium oxide photocatalysts operating under visible light irradiation, J. Catal. 216 (2003) 505–516.
[9] J.H. Mo, Y.P. Zhang, Q.J. Xu, Y.F. Zhu, J.J. Lamson, R.Y. Zhao, Determination, risk assessment of by-products resulting from photocatalytic oxidation of toluene, Appl. Catal. B 89 (2009) 570–576.
[10] J. Bandara, U. Klehm, J. Kiwi, Raschig rings-Fe_2O_3 composite photocatalyst activate in the degradation of 4-chlorophenol and Orange II under daylight irradiation, Appl. Catal. B 76 (2007) 73–81.
[11] W. Ketir, A. Bouguelia, M. Trari, Photocatalytic removal of M^{2+} (=Ni^{2+}, Cu^{2+}, Zn^{2+}, Cd^{2+}, Hg^{2+} and Ag^{+}) over new catalyst $CuCrO_2$, J. Hazard. Mater. 158 (2008) 257–263.
[12] X.L. Fu, X.X. Wang, Z.X. Ding, D.Y.C. Leung, Z.Z. Zhang, J.L. Long, W.X. Zhang, Z.H. Li, X.Z. Fu, Hydroxide $ZnSn(OH)_6$: a promising new photocatalyst for benzene degradation, Appl. Catal. B 91 (2009) 67–72.
[13] J.R. Xiao, T.Y. Peng, R. Li, Z.H. Peng, C.H. Yan, Preparation, phase transformation and photocatalytic activities of cerium-doped mesoporous titania nanoparticles, J. Solid State Chem. 179 (2006) 1161–1170.
[14] Y.H. Xu, H.R. Chen, Z.X. Zeng, B. Lei, Investigation on mechanism of photocatalytic activity enhancement of nanometer cerium-doped titania, Appl. Surf. Sci. 252 (2006) 8565–8570.
[15] S. Yuan, Y. Chen, L.Y. Shi, J.H. Fang, J.P. Zhang, J.L. Zhang, H. Yamashita, Synthesis and characterization of Ce-doped mesoporous anatase with long-range ordered mesostructure, Mater. Lett. 61 (2007) 4283–4286.
[16] V. Stengl, S. Bakardjieva, N. Murafa, Preparation and photocatalytic activity of rare earth doped TiO_2 nanoparticles, Mater. Chem. Phys. 114 (2009) 217–226.
[17] M.D. Hernandez-Alonso, A.B. Hungria, A. Martinez-Arias, M. Fernandez-Garcia, J.M. Coronado, J.C. Conesa, J. Soria, EPR study of the photoassisted formation of radicals on CeO_2 nanoparticles employed for toluene photooxidation, Appl. Catal. B 50 (2004) 167–175.
[18] S. Song, L.J. Xu, Z.Q. He, J.M. Chen, Mechanism of the photocatalytic degradation of C.I. Reactive Black 5 at pH 12.0 using $SrTiO_3$/CeO_2 as the catalyst, Environ. Sci. Technol. 41 (2007) 5846–5853.
[19] Y.Q. Zhai, S.Y. Zhang, H. Pang, Preparation, characterization and photocatalytic activity of CeO_2 nanocrystalline using ammonium bicarbonate as precipitant, Mater. Lett. 61 (2007) 1863–1866.
[20] P.F. Ji, J.L. Zhang, F. Chen, M. Anpo, Study of adsorption and degradation of acid orange 7 on the surface of CeO_2 under visible light irradiation, Appl. Catal. B 85 (2009) 148–154.
[21] Y.B. Xie, C.W. Yuan, Visible-light responsive cerium ion modified titania sol and nanocrystallites for X-3B dye photodegradation, Appl. Catal. B 46 (2003) 251–257.
[22] T. Cordero, C. Duchamp, J.M. Chovelon, C. Ferronato, J. Matos, Influence of L-type activated carbons on photocatalytic activity of TiO_2 in 4-chlorophenol photodegradation, J. Photochem. Photobiol. A 191 (2007) 122–131.
[23] J.M. Herrmann, J. Matos, J. Disdier, C. Guillard, J. Laine, S. Malato, J. Blanco, Solar photocatalytic degradation of 4-chlorphenol using the synergistic effect between titania and activated carbon in aqueous suspension, Catal. Today 54 (1999) 255–265.
[24] J. Matos, J. Laine, J.M. Herrmann, Synergy effect in the photocatalytic degradation of phenol on a suspended mixture of titania and activated carbon, Appl. Catal. B 18 (1998) 281–291.
[25] Y.P. Cheng, H.Q. Sun, W.Q. Jin, N.P. Xu, Photocatalytic degradation of 4-chlorophenol with combustion synthesized TiO_2 under visible light irradiation, Chem. Eng. J. 128 (2007) 127–133.
[26] M.L. Satuf, R.J. Brandi, A.E. Cassano, O.M. Alfano, Photocatalytic degradation of 4-chlorophenol: a kinetic study, Appl. Catal. B: Environ. 82 (2008) 37–49.